Molecular Biology of the Cell
Vol. 4, 1189–1204, November 1993

The Gly/Arg-rich (GAR) Domain of *Xenopus* Nucleolin Facilitates In Vitro Nucleic Acid Binding and In Vivo Nucleolar Localization

Mary A. Heine, Michele L. Rankin, and Patrick J. DiMario

Department of Biochemistry, Louisiana State University, Baton Rouge, Louisiana 70810

Submitted March 24, 1993; Accepted September 21, 1993

Epitope-tagged *Xenopus* nucleolin was expressed in *Escherichia coli* cells and in *Xenopus* oocytes either as a full-length wild-type protein or as a truncation that lacked the distinctive carboxy glycine/arginine-rich (GAR) domain. Both full-length and truncated versions of nucleolin were tagged at their amino termini with five tandem human c-*myc* epitopes. Whether produced in *E. coli* or in *Xenopus*, epitope-tagged full-length nucleolin bound nucleic acid probes in in vitro filter binding assays. Conversely, the *E. coli*–expressed GAR truncation failed to bind the nucleic acid probes, whereas the *Xenopus*-expressed truncation maintained slight binding activity. Indirect immunofluorescence staining showed that *myc*-tagged full-length nucleolin properly localized to the dense fibrillar regions within the multiple nucleoli of *Xenopus* oocyte nuclei. The epitope-tagged GAR truncation also translocated to the oocyte nuclei, but it failed to efficiently localize to the nucleoli. Our results show that the carboxy GAR domain must be present for nucleolin to efficiently bind nucleic acids in vitro and to associate with nucleoli in vivo.

INTRODUCTION

Vertebrate nucleolin is a nucleolar specific phosphoprotein of 90–110 kDa that is believed to quickly associate with nascent preribosomal RNA within the dense fibrillar regions of nucleoli (reviewed by Olson, 1990; Escande *et al.*, 1985; Herrera and Olson, 1986). Nucleolin is abundant in rapidly dividing somatic cells (Orrick *et al.*, 1973) and amphibian oocytes (Caizergues-Ferrer *et al.*, 1989; DiMario and Gall, 1990) where rates of ribosome production are maximal. Herrera and Olson (1986) demonstrated that the majority of nucleolin rapidly associates with newly synthesized pre-ribosomal RNA, and recent studies on the yeast nucleolin-like NSR1 protein showed that 35S preribosomal RNA processing and ribosome biogenesis were impaired when the NSR1 protein was eliminated in a *nsr1* deletion strain (Kondo *et al.*, 1992a,b). This combined evidence suggests that nucleolin plays an early role in the processing of preribosomal RNA or in the preassembly of ribosomes (Olson, 1990).

Nucleolin is a modular protein (Olson, 1990). Its amino terminal third consists of alternating basic and acidic domains, and the carboxy terminal two-thirds consists of four RNA-binding domains followed by a glycine- and N^G,N^G dimethylarginine-rich (GAR) domain (Lischwe *et al.*, 1985; Lapeyre *et al.*, 1986). The amino terminal acidic domains have been implicated in binding histone H1 to decondense rDNA for transcription (Erard *et al.*, 1988, 1990) or in binding basic ribosomal proteins to facilitate ribosome assembly (Olson, 1990). On the other hand, the amino terminal basic domains have been implicated in binding upstream rDNA sequences to regulate rRNA gene expression (Olson *et al.*, 1983). The four RNA-binding domains are similar to those found in several other RNA-binding proteins such as the heterogeneous nuclear ribonucleoproteins (hnRNPs), poly(A)-binding proteins, and ribonucleoproteins specifically associated with U1 and U2 small nuclear (sn) RNAs (reviewed by Dreyfuss *et al.*, 1993). For example, the RNA-binding domain of the U1 snRNP A protein can bind RNA in vitro (Query *et al.*, 1989), and its crystal structure provides evidence for likely interactions with stem-loop II of U1 snRNA (Nagai *et al.*, 1990). On the basis of what is already known about these RNA-binding domains in other proteins, we can assume that some or all of nucleolin's four RNA-binding domains are important for observed in vitro RNA and DNA interactions (Olson *et al.*, 1983; Bugler *et al.*, 1987; Sapp *et al.*, 1989). However, specific in vivo interactions between nucleolin's four RNA-

binding domains and pre-rRNA have yet to be determined.

Just downstream of the fourth RNA-binding domain is the GAR domain that is referred to as the Arg-Gly-Gly (RGG) box by Dreyfuss *et al.* (1993) for other RNA-binding proteins. Ghisolfi *et al.* (1992) have shown that this domain consists of repeated β-turns that confer an overall helical structure on this domain (i.e. a β-spiral), and they have shown that this basic domain binds RNA or DNA independently of the four upstream RNA-binding domains. The GAR domain may nonspecifically bind preribosomal RNA to perhaps unwind secondary structures thereby facilitating more specific interactions between nucleolin and preribosomal RNA (Ghisolfi *et al.*, 1992). Despite these predictions, the in vivo functions and associations of this GAR domain also remain unknown.

To gain more information about individual domains of nucleolin, specifically the carboxy GAR domain, we have epitope-tagged *Xenopus* nucleolin at its amino terminus and truncated the protein just before the GAR domain. Here we show that the tagged truncation produced in *Escherichia coli* no longer binds radiolabeled nucleic acids in vitro and that the tagged truncation produced in *Xenopus* oocytes fails to efficiently localize to the multiple nucleoli in vivo.

MATERIALS AND METHODS

Recovery of Xenopus Nucleolin cDNAs

The polymerase chain reaction (PCR) was used as described (Frohman *et al.*, 1988) to recover full length *Xenopus* nucleolin cDNAs. Briefly, *Xenopus* ovary RNA was purified as described (Epstein *et al.*, 1986), and poly(A)+ mRNA was further enriched by oligo d(T) chromatography (Kingston, 1993). To synthesize negative cDNA strands, 1 μg of poly(A)+ RNA was reverse transcribed using a cDNA Synthesis System Plus kit (Amersham, Arlington Heights, IL) according to the manufacturer's recommended protocol. A *Xenopus* nucleolin-specific oligonucleotide was used in the PCR as the 5′ primer for the synthesis of positive nucleolin cDNA strands. This primer was homologous to nucleotides 28–57 of an incomplete *Xenopus* nucleolin cDNA (Caizergues-Ferrer *et al.*, 1989) except that nucleotides 34 (G) and 35 (C) were changed to C and T, respectively to provide a *Hin*dIII site for cloning purposes. The 3′ oligonucleotide primer contained poly (dT) at its 5′ end and *Xho*I, *Sal*I, and *Cla*I restriction sites at its 3′ end for subsequent cloning. The PCR cycles were carried out essentially as described (Frohman *et al.*, 1988) using a Perkin-Elmer-Cetus DNA Thermal Cycler (Norwalk, CT) and *Taq*I polymerase. A predicted PCR product of ~2000 base pairs (bp) was gel purified, cut with *Hin*dIII and *Xho*I to generate sticky ends, and ligated into a pBluescript vector (Stratagene, La Jolla, CA) at the appropriate polylinker sites. The PCR product was determined to encode nucleolin by sequence analysis using a dideoxy Sequenase kit (United States Biochemicals, Cleveland, OH).

A 645-bp *Hin*dIII/*Eco*RI fragment from the 5′ end of the PCR product was used to screen a *Xenopus* ovary cDNA lambda-ZAP library (Stratagene). Several positive cDNA clones were selected on the basis of size and three previously identified internal *Eco*RI sites (Caizergues-Ferrer *et al.*, 1989). Single- and double-stranded sequencing techniques were used to further characterize several of these cDNAs. Two cDNAs, *Xl*C23-92 and *Xl*C23-56, were completely sequenced as described. Their sequences overlap and a full-length nucleolin cDNA was constructed by ligating the two cDNAs at a common *Xba*I site shown in Figure 1. The EMBL accession number for this full length nucleolin cDNA is X63091.

Computer Sequence Analysis

Analyses of the *Xenopus* nucleolin cDNA sequence and the deduced protein sequence were performed using the University of Wisconsin Genetics Computer Group Sequence Analysis Software Package, Version 7.1 (Devereux *et al.*, 1984).

cDNA Subcloning and Mutagenesis

A 13–amino acid segment of the human c-*myc* protein has been used successfully as an epitope to tag cellular proteins (Monro and Pelham, 1986). Six tandem repeats of the DNA encoding the *myc* epitope were subsequently constructed and cloned downstream of the T3 promoter of pBluescript by Roth *et al.* (1991). For our studies the 5′ end of the nucleolin coding sequence was ligated to the 3′ end of the fifth tandem *myc* DNA repeat by using common *Nco*I sites, one shortly downstream of the fifth *myc* tag and the other at the predicted ATG translation start codon of the nucleolin cDNA. Ligation between the *myc* and nucleolin cDNA sequences placed 5 tandem *myc* repeats upstream and in frame with the nucleolin ATG start codon. The fifth *myc* repeat unit was followed by an additional eight nonnucleolin amino acids (MESLGDLT) and then the initial methionine of nucleolin. Although the nucleolin ATG start codon was left intact, each *myc* DNA repeat begins with its own ATG translation start codon. The β-gal promoter of pBluescript was upstream of the T3 promoter, and it permitted bacterial expression of the *myc*-tagged fusion protein. The resulting *myc*-nucleolin construct is referred to as p*myc-Xl*C23.

The *Xl*C23-56 cDNA that was used to construct p*myc-Xl*C23 contains the 3′ untranslated region, but it has no poly(A) sequence. To ensure stability of oocyte-injected mRNA, the 3′ untranslated region of *Xenopus* NO38 cDNA with a poly(A) tail of 59 residues was used to replace most of the nucleolin 3′ untranslated region of p*myc-Xl*C23. Specifically, the 3′ untranslated region of the NO38 cDNA was excised by cutting at an *Eco*RV site that had been engineered within the 3′ untranslated region (construct C11 of Peculis and Gall, 1992) and at a downstream *Sac*I polylinker site. The resulting 400-bp NO38 fragment was ligated to p*myc-Xl*C23 that had been first cut with *Spe*I; its ends made flush with the Klenow polymerase fragment and then cut again at a downstream *Sac*I polylinker site. The resulting plasmid is called p*myc-Xl*C23-NO38. *E. coli* and *Xenopus* oocyte translation products, derived from p*myc-Xl*C23-NO38, are depicted in Figure 1, A and B, respectively.

The carboxy terminus of nucleolin was truncated upstream of the GAR domain by cutting p*myc-Xl*C23-NO38 at the unique *Xba*I site (Figure 1), filling in the overhangs with the Klenow polymerase fragment and then religating the plasmid. This procedure introduced four extra base pairs that shifted the reading frame such that the original nucleolin sequence of -L_{573}DFAKPKG_{580}- (where G_{580} is 4 residues upstream of the GAR domain) was changed to -L_{573}ARLCKT*. The (*) denotes a newly created stop codon that is positioned less than four codons upstream of the GAR-encoding DNA sequence. Sequence analysis verified the predicted mutagenesis, and the resulting plasmid is referred to as p*myc-Xl*C23δGAR. *E. coli* and *Xenopus* oocyte translation products, derived from p*myc-Xl*C23δGAR, are depicted in Figure 1, C and D, respectively.

Bacterial Expression

The protease deficient *E. coli* strain, BL21 (Sturdier *et al.*, 1990), and the recombination deficient *E. coli* strain, XL1-Blue, were transformed with cesium chloride-banded p*myc-Xl*C23-NO38 or p*myc-Xl*C23δGAR. The BL21 was cotransformed with pUBS520 (from Dr. R. Mattes, Institut fur Industrielle Genetik, Universitat Stuttgart, Stuttgart). pUBS 520 is a derivative of pACYC 177 that was modified to contain the *E. coli* $lacI_q$ gene that encodes the lac repressor to prevent weak constitutive expression from lactose inducible promoters.

pUBS520 also carries the *argU* (formerly called *dnaY*) gene of *E. coli* (Brinkman *et al.*, 1989) for high level fusion protein expression. Fusion protein expression was induced with isopropyl β-D-thiogalactopyranoside (IPTG) once cultures had reached an OD_{600} of 0.5 at 37°C. Cells were allowed to express fusion protein for 3 h at 37°C with vigorous shaking after which the cells were pelleted, resuspended in 0.5 ml of sodium dodecyl sulfate (SDS)-sample buffer (Laemmli, 1970), and lysed by sonication. Samples were boiled for 5 min and then clarified by centrifugation. *E. coli*-expressed translation products derived from p*myc-XlC23-NO38* or p*myc-XlC23δGAR* are depicted in Figure 1, A and C, respectively.

Oocyte Injections

An unique *Bam*HI site downstream of the poly(A) sequence of p*myc-XlC23-NO38* and p*myc-XlC23δGAR* permitted linearizing the plasmid for in vitro runoff transcription. RNA transcripts were synthesized from the T3 promoter positioned upstream of the *myc* tags. The reaction mixture contained 2 μg of linearized template DNA, 0.75 mM each of the ribonucleotides CTP, UTP, and ATP, and 0.5 mM GTP. The diguanosine triphosphate cap analogue (New England Bio Labs, Beverly, MA) was included at 0.75 mM. One microliter of undiluted T3 polymerase (Stratagene) was used for transcription along with appropriately diluted buffers and salts that were supplied with the polymerase. The volume of the reaction mixture was 20 μl. RNA synthesis occurred at 37°C for 1 h, after which 0.5 μg of RNase-free DNase (BRL, Gaithersburg, MD) was added. Template DNA was digested at 37°C for 15 min. The mixture was then adjusted to 100 μl with the addition of distilled water, adjusted to a final concentration of 300 mM sodium acetate, and then extracted with phenol/chloroform. RNA transcripts were precipitated with ethanol, pelleted by centrifugation, washed with 70% ethanol, vacuum dried, and then dissolved in distilled water to ~1 mg/ml for oocyte injection. RNA integrity was assayed by Northern blot analysis as described by Epstein *et al.* (1986). *Xenopus*-expressed translation products that were derived from p*myc-XlC23-NO38* or p*myc-XlC23δGAR* are depicted in Figure 1, B and D, respectively.

Female *Xenopus* frogs were purchased from Xenopus I (Ann Arbor, MI). Individual oocytes were removed from ovary and incubated for 1 h in OR2 medium at 18°C before mRNA injection. OR2 medium is 82.5 mM NaCl, 2.5 mM KCl, 1.0 mM $CaCl_2$, 1.0 mM $MgCl_2$, 1.0 mM Na_2HPO_4, and 5.0 mM *N*-2-hydroxyethylpiperazine-*N'*-2-ethanesulfonic acid (Wallace *et al.*, 1973). Messenger RNA encoding *myc*-tagged nucleolin fusion protein was injected into stages 5 and 6 oocytes. After injection the oocytes were incubated in OR2 medium at 18°C for 18–24 h. The nuclear contents consisting of lampbrush chromosomes, multiple nucleoli, and RNP particles were prepared for immunofluorescence microscopy by the procedures of Gall *et al.* (1991). Specifically, oocyte nuclei were individually hand isolated in freshly prepared 5:1 isolation medium (83 mM KCl, 17 mM NaCl, 1.0 mM Mg^{+2}, and 10 mM tris(hydroxymethyl)aminomethane [Tris] pH 7.2). A nucleus was cleaned of cytoplasm by drawing it up and down in a pulled Pasteur pipette after which the nuclear envelope was removed with No. 5 Dumont (Regine, Switzerland) forceps. The nuclear contents remain as a gelatinous plug in this 5:1 isolation buffer. The plug was then transferred by pipette to "quarter strength" dispersal medium (20.75 mM KCl, 4.25 mM NaCl, 2.5 mM Tris pH 7.2, with 0.1% paraformaldehyde, 0.5–1.0 mM $MgCl_2$, and 5–10 μM $CaCl_2$) for ~30 sec and then to a droplet of fresh dispersal medium placed into a well that was constructed on a protein-coated microscope slide (for details see Gall *et al.*, 1991). The Mg^{+2} and Ca^{+2} concentrations in this spreading medium were adjusted within the indicated ranges to ensure consistent dispersal from one batch of oocytes to the next. For example, decreasing the Mg^{+2} concentration and increasing the Ca^{+2} concentration facilitates dispersal, whereas increasing the Mg^{+2} concentration and decreasing the Ca^{+2} concentration impedes dispersal (Gall *et al.*, 1991). Without proper dispersal, the nuclear contents remain as a condensed gelatinous plug, and we have noted that the nucleoli do not stain well with various anti-nucleolin antibodies (see below) under these conditions. Once in dispersal medium, the nuclear contents were allowed to settle onto the slides and spread. To permanently affix the nuclear contents to the glass, the slides were centrifuged at 4500 rpm for 1 h in a Sorvall HS4 rotor (Newton, CT) that was equipped with specially built slide carriers (see Gall *et al.*, 1991). The nuclear preparations were then fixed with 2% paraformaldehyde in phosphate-buffered saline (PBS) that contained 1 mM $MgCl_2$. The final preparations were blocked with 10% horse serum in PBS and then probed with various antibodies.

Total Nuclear Proteins, Gel Electrophoresis, and Southwestern Analysis

Nuclear proteins were prepared from hand isolated oocyte nuclei that were stripped of clinging cytoplasm by pipetting up and down (Roth and Gall, 1987). SDS-polyacrylamide gel electrophoresis was according to Laemmli (1970). Two-dimensional (2-D) isoelectric focusing of oocyte nuclear proteins was as described (DiMario and Gall, 1990). Western blots were probed with labeled, heat denatured DNA ("Southwesterns") as previously described (DiMario *et al.*, 1989).

Nucleolin Purification and Antiserum Production

Nucleolin was purified from S100 extracts of *Xenopus* kidney cells (X1K2) by anion exchange chromatography and poly[G]-agarose chromatography. The extract was prepared according to the procedures of McStay and Reeder (1986, 1990). In the purification of nucleolin, an aliquot (17 ml) of cell extract was applied to DEAE-Sepharose (DCL-6B-100, Sigma, St. Louis, MO) packed in a 20 × 1.5 cm I.D. BioRad Econo column Richmond, CA. The beads had been previously equilibrated in column buffer (20 mM Tris · HCl pH 6.2, 6 M urea, 1 mM dithiothreitol, and 1 mM EDTA). A linear gradient of NaCl (0.0–0.75 M, 350 ml total volume) passed through the column at 4°C. Each fraction (5.6 ml) was monitored by A_{223} and A_{280} to establish a column elution profile. Fraction aliquots (0.25 ml) were precipitated with 1 ml of acetone, and the pellets were resuspended in 50 μl of SDS sample buffer (Laemmli, 1970). Fractions were resolved on a 10% polyacrylamide SDS gel, transferred to nitrocellulose, and probed with monoclonal antibody (mAb) G1C7 and secondary reagents from the Vectastain detection kit (Vector Laboratories, Burlingame, CA). Nucleolin typically eluted from the cellulose diethylaminoethyl-cellulose (DEAE) column at ~0.35 M NaCl. Those fractions enriched for nucleolin were dialyzed overnight in poly[G] column buffer (50 mM Tris base pH 7.9, 5 mM $MgCl_2$, and 1 mM EDTA) at 4°C. Dialyzed fractions were loaded onto a 5 ml poly[G]-agarose resin (P1908, Sigma) that had been packed in a 9 × 1.5 cm I.D. BioRad Econo column and equilibrated with poly[G] column buffer. A linear gradient of KCl (0.0–1.0 M, total volume of 140 ml) was passed through the column at 4°C. The flow rate was slowed to 0.35 ml/min using a peristaltic pump. Fractions of 3 ml were collected and the A_{223} and A_{280} were again read for each fraction to obtain a column elution profile. Aliquots (0.5 ml) of the fractions were precipitated with 2 ml of 100% acetone and pelleted. Pellets were resuspended in 50 μl of SDS sample buffer, and individual fractions were resolved on a 10% polyacrylamide SDS gel. Polyacrylamide gels were silver stained to determine which fractions contained only nucleolin. Nucleolin typically eluted from the poly[G]-agarose column at ~0.75 M KCl.

Purified nucleolin was next transferred to sterile PBS and condensed using an Amicon condenser (Dancers, MA) and Millipore spin columns (Bedford, MA) to a final volume of 0.2 ml. The protein sample was then emulsified with 0.2 ml of Freund's complete adjuvant (F-4258, Sigma) and injected subcutaneously into a female New Zealand white rabbit. The rabbit was boosted twice; each boost used Freund's incomplete adjuvant (F-5506, Sigma), and each boost was administered 3 weeks after the previous injection. The resulting polyclonal serum (R2D2) was characterized for anti-nucleolin specificity by probing Western blots that contained a complex mixture of cellular proteins (Figure 5B).

Other Antibodies

Mouse mAb 9E10 was originally developed by Evan *et al.* (1985); it labels the *myc* repeat peptide used to tag nucleolin. Mouse mAb G1C7 was developed by Rabiya Tuma and Mark Roth at the Fred Hutchinson Cancer Research Center, Seattle, WA; it labels both versions of *Xenopus* nucleolin and a larger unidentified protein of approximately 180 kDa on Western blots. A Vectastain ABC kit (Vector Laboratories) was used to immunochemically detect mAbs 9E10 and G1C7 on western blots. Anti-fibrillarin mouse mAb 72B9 was originally developed by K. Michael Pollard, and it was characterized by Reimer *et al.* (1987). For fluorescence microscopy, affinity-purified, fluorescein-coupled goat anti-mouse IgG (Cappel, West Chester, PA) and affinity-purified, rhodamine-coupled mouse anti-rabbit IgG (Pierce, Rockford, IL) were used to detect the respective primary antibodies within *Xenopus* nuclear preparations.

RESULTS

Two partial but overlapping *Xenopus* nucleolin cDNAs (*Xl*C23-92 and *Xl*C23-56) were ligated together at their common *Xba*I sites (bp 1779–1784) to provide a complete coding sequence of 2424 bp (EMBL accession number X63091). This sequence includes 63 bp of 5′ untranslated DNA and 407 bp of 3′ untranslated DNA. The translation start codon is nucleotides 64–66, and it is well defined by Kozak's criteria for translation initiation (Kozak, 1987). An upstream TAG stop codon at nucleotides 19–21 is in frame with the ATG start codon This supports the probability that the entire protein coding sequence is present. The translation stop codon is at nucleotides 2017–2019, and the deduced protein is 651 amino acids in length (Figure 1A). Its calculated molecular weight is 70 110 Da. Two *Xenopus* nucleolin proteins display apparent molecular weights of 90 and 95 kDa on SDS-gels (Caizergues-Ferrer *et al.*, 1989; DiMario and Gall, 1990). Their migrations are anomalous because of the overall acidic charge of *Xenopus* nucleolin (calculated pI = 4.65; observed pI = 5.0–5.2) (DiMario and Gall, 1990). Other proteins that show anomalous migrations on SDS-gels include nucleoplasmin (Dingwall *et al.*, 1987), the RNA-binding hnRNP proteins C1/C2 (Swanson *et al.*, 1987), and the RNA-binding protein of the fragile X gene, *FMR1* (Siomi *et al.*, 1993). All have acidic stretches like nucleolin.

The amino terminal third of *Xenopus* nucleolin is a modular composition of alternating basic and acidic domains (Figure 1), as in chicken (Maridor and Nigg, 1990) and Chinese hamster ovary (CHO) nucleolin (Lapeyre *et al.*, 1987). Although shorter in overall length, the amino terminal region of *Xenopus* nucleolin contains five acidic domains and six basic domains, rather than four acidic and five basic domains as found in chicken and CHO nucleolin. As in other vertebrate versions of nucleolin, the carboxy two-thirds of *Xenopus* nucleolin consists of four RNA-binding domains, a GAR domain, and finally a short tail of seven amino acids (Figure 1A).

Wild-Type Xenopus Nucleolin Expression in E. coli

A 13–amino acid fragment of human c-*myc* (MEQKLISEEDLNE) has been used successfully to epitope tag several different proteins and then to localize these proteins within cell compartments (Monro and Pelham, 1986, 1987; Pelham *et al.*, 1988). Six DNA repeats encoding the *myc* tag were cloned into pBluescript downstream of the β-galactosidase and T3 promoters by Roth *et al.* (1991). Induction of the β-galactosidase promoter in *E. coli* with IPTG should produce a fusion protein of 751 amino acids that consists of a small lacZ peptide, five *myc*-tags, the eight amino acid linker, and then nucleolin. Figure 1A depicts this entire *E. coli* fusion protein.

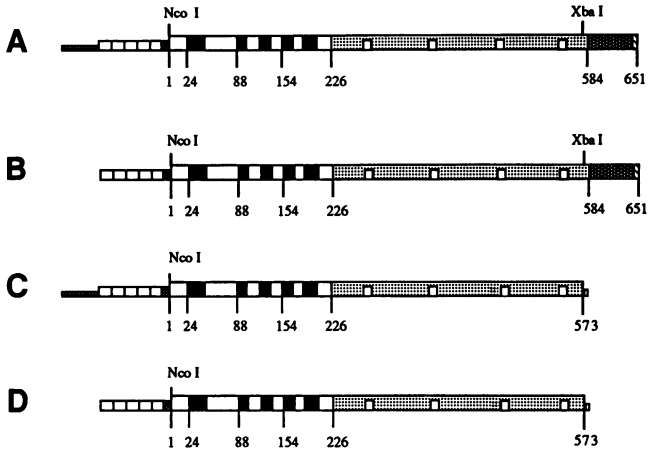

Figure 1. Bar diagrams showing various fusion proteins of *Xenopus* nucleolin. (A) The fusion protein expressed in *E. coli* after IPTG induction from either p*myc*-*Xl*C23 or p*myc*-*Xl*C23-NO38. Starting from the left, the fusion consists of a portion of lacZ (1/2 width checkered box), five *myc* tags (3/4 width white boxes), and a linker region (3/4 width checkered box). Nucleolin is shown as a series of full-width boxes: the amino terminal third of *Xenopus* nucleolin consists of alternating basic domains (□) and acidic domains (■). The carboxy terminal two-thirds of nucleolin consists of four RNA-binding domains each containing an RNP consensus sequence (small white insets). The fourth RNA-binding domain is followed by a GAR domain (□) and then a tail of seven amino acids (▨). (B) The full-length fusion protein expressed in *Xenopus* oocytes from injected mRNA that was in vitro transcribed from p*myc*-*Xl*C23-NO38. Translation initiation should have occurred at the initial methionine codon of the first *myc* tag. (C) The GAR truncation expressed in *E. coli* after IPTG induction of the β-gal promoter of p*myc*-*Xl*C23δGAR. The GAR domain and the short carboxy tail were removed by creating a stop codon shortly before the GAR-encoding cDNA by mutagenizing p*myc*-*Xl*C23-NO38 at the *Xba*I site. (D) The GAR truncation expressed from p*myc*-*Xl*C23δGAR in *Xenopus* oocytes from injected mRNA that was in vitro transcribed from p*myc*-*Xl*C23δGAR.

Endogenous nucleolin from vertebrate cells can be observed simply by probing western blots with radiolabeled, single-stranded DNA (DiMario and Gall, 1990). We have used this filter binding assay in the studies reported here not to define in vivo functions but rather to monitor nucleolin's production in *E. coli* and to test the potential of wild-type nucleolin and various mutations of nucleolin to bind DNA under a set of defined in vitro conditions. Figure 2A shows a Western blot that was probed with radiolabeled single-stranded DNA to

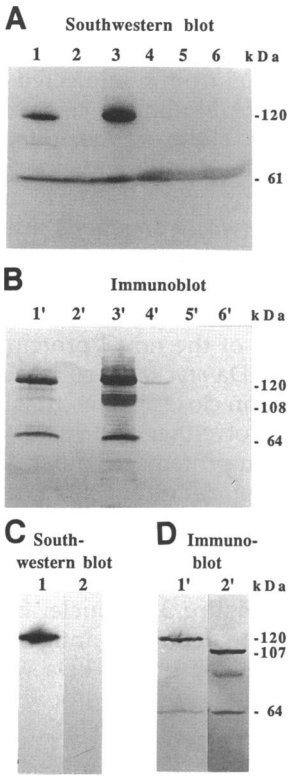

Figure 2. Western blots displayed *myc*-tagged nucleolin fusion proteins expressed in *E. coli*. (A) The blot was probed with radiolabeled single-stranded DNA. Lanes 1 and 2 contain lysate proteins from protease deficient BL21 cells that had been transformed with p*myc*-*Xl*C23. The predicted fusion protein should consist of a short lacZ peptide, the *myc* tags, and the entire *Xenopus* nucleolin protein. A prominent DNA-binding protein of 120 kDa was found only in the induced cells (lane 1) but not the noninduced cells (lane 2). Lanes 3 and 4 contain lysate proteins from XL1-Blue cells that had been transformed with p*myc*-*Xl*C23. A prominent DNA-binding protein of 120 kDa again was found only in the IPTG induced cells (lane 3) and not in the noninduced cells (lane 4). Control lanes 5 and 6 contain lysate proteins from XL1-Blue cells that had been transformed with p3A10-positive (see text). However, no novel DNA-binding proteins were observed from induced (lane 5) or noninduced (lane 6) cells. The DNA-binding protein of 61 kDa was found in all three transformants whether they were induced or not. (B) The blot used for A was reprobed with mAb 9E10 that was detected immunochemically. Lane 1′ contains antigens of 120 and 64 kDa from induced protease deficient BL21 cells. The 120-kDa antigen comigrated with the DNA-binding protein shown in A. No antigens were detected in the noninduced BL21 cells (lane 2′). Besides the 120- and 64-kDa antigens, abundant antigens of ~108 kDa were observed in extracts of induced XL1-Blue cells (lane 3′). No antigens were observed in cells harboring p3A10-positive (lanes 5′ and 6′). (C) Southwestern blots were used to characterize the *E. coli*-expressed GAR truncation. Lane 1: *myc*-tagged full-length nucleolin fusion protein was expressed in *E. coli* as a positive control for nucleic acid binding and as a molecular weight standard by which to compare the GAR truncation. Lane 2: the GAR truncation was not detected by Southwestern assay. (D) The filters used in C were reprobed with mAb 9E10. Although no binding proteins were detected in C, lane 2, the GAR truncation was present within the extract as detected by mAb 9E10 (lane 2′).

detect *E. coli*-produced nucleolin fusion proteins. Lanes 1 and 2 contain proteins from the protease deficient BL21 strain of *E. coli* (Sturdier *et al.*, 1990) that was transformed with p*myc*-*Xl*C23. A novel DNA-binding protein of 120 kDa was observed in extracts of IPTG-induced cells (Figure 2A, lane 1), but no DNA-binding protein of this weight was found in extracts of the same cells that were not induced (Figure 2A, lane 2).

A nonprotease deficient *E. coli* strain, XL1-Blue, was also transformed with p*myc*-*Xl*C23. The 120-kDa, DNA-binding protein was again observed in this strain only after IPTG induction (Figure 2A, lanes 3 and 4). As a negative control, *E. coli* cells were transformed with a Bluescript-based plasmid containing a newt cDNA insert that when induced with IPTG, produces a fusion protein that is detectable with mAb 3A10, an anti-histone H1 antibody (DiMario and Gall, 1990). This plasmid, referred to simply as p3A10-positive, failed to produce a novel DNA-binding protein either with or without IPTG induction (Figure 2A, lanes 5 and 6, respectively). A prominent single-stranded DNA-binding protein of 61 kDa was observed in all *E. coli* lysates whether the lysates were prepared from induced or noninduced cells, and whether or not they contained plasmids encoding nucleolin (Figure 4A, lanes 1–6). Because of its presence in all *E. coli* lysates, we were confident that the 61 kDa was not a proteolytic fragment of the 120 kDa DNA-binding protein (see below).

The apparent molecular weight of the 120 kDa DNA-binding protein and its presence only in lysates of induced cells strongly indicated that it was the nucleolin fusion protein. To test this we used mAb 9E10 that reacts well with the *myc* epitope (Evan *et al.*, 1985). Figure 2B shows the same blot that was used in Figure 2A, but after it was reprobed with mAb 9E10. The primary 9E10 antibody was detected by immunochemical staining. The prominent antigen of Figure 2B, lane 1′ co-migrated with the 120 kDa DNA-binding protein observed in Figure 2A, lane 1. Because the 120-kDa antigen was found only in cells harboring p*myc*-*Xl*C23 and after IPTG induction, we concluded that this antigen is the *myc*-tagged version of intact *Xenopus* nucleolin.

mAb 9E10 also labeled a protein of 64 kDa that was found only in p*myc*-*Xl*C23–transformed cells after IPTG induction. Because it was detected by virtue of the epitope-tags, the 64-kDa protein must have been the amino terminal fragment of nucleolin. Although we could not rule out premature translation termination as cause for its presence, the 64-kDa protein was probably a proteolytic fragment of the 120-kDa antigen. Although similar in size, this 64-kDa antigen migrated slightly behind the 61-kDa *E. coli*-specific DNA-binding protein shown in Figure 2A. Because we were able to resolve the 61-kDa DNA-binding from the 64-kDa antigen on the gradient polyacrylamide gels in Figure 2, we were confident that the 64-kDa antigen was not related to the smaller *E. coli*-specific nucleic acid-binding protein.

In addition to the intact 120-kDa and truncated 64-kDa antigens, several other proteolytic fragments of ~108 kDa were observed in lysates prepared from induced XL1-Blue cells that contained p*myc*-*Xl*C23 (Figure 2B, lane 3'). The *myc* tags were still present at their amino termini. Therefore, proteolysis had to occur at the carboxy end of the proteins. Simply on the basis of apparent molecular weights, the difference in size between the intact 120-kDa fusion protein and these 108-kDa fragments suggested that ~9% of the intact fusion protein was missing. Although the GAR domain and the very carboxy tail actually constitute 9% of the overall linear length of the *E. coli*-expressed fusion protein (68 out of 751 total amino acid residues), these crude estimates merely suggested that the GAR domain was missing from the 108-kDa antigens.

To test if the GAR domain is required for in vitro DNA-binding activity, we truncated the fusion protein by engineering a stop codon in the p*myc*-*Xl*C23-NO38 expression plasmid at an unique *Xba* I site (compare Figure 1, A and C). The resulting plasmid, p*myc*-*Xl*C23δGAR, was expressed in *E. coli*. Labeling with mAb 9E10 showed that the tagged GAR truncation was indeed present within the cell lysate (Figure 2D, lane 2'). However, it failed to bind radiolabeled DNA (Figure 2C, lane 2). The truncation's apparent molecular weight of 107 kDa was in good agreement with the predicted loss of ~9% of the intact fusion protein of 120 kDa (Figure 2, C and D, lanes 1 and 1'). Failure to bind the probe under these conditions suggested that the GAR domain must either bind nucleic acids directly as suggested by Ghisolfi *et al.* (1992) or regulate the conformational state of other nucleic acid binding domains within nucleolin by intramolecular peptide-peptide interactions.

Xenopus Oocyte Expression

The in vitro binding results with fusion proteins produced in *E. coli* only suggested potential nucleic acid interactions that may be important for nucleolin association within the nucleoli for preribosomal RNA processing or perhaps ribosome assembly and transport. To approach possible in vivo associations and functions, we produced epitope-tagged versions of nucleolin that were either full length (Figure 1B) or deleted for the carboxy GAR domain (Figure 1D) in *Xenopus* oocytes. These tagged proteins were produced by injecting mRNAs that were in vitro synthesized from p*myc*-*Xl*C23-NO38 or p*myc*-*Xl*C23δGAR, respectively. Both mRNAs were synthesized using the T3 promoter just upstream of the *myc*-tags. Therefore, unlike translation initiation in *E. coli*, translation initiation in *Xenopus* oocytes should have occurred at the initial AUG codon of the first *myc* tag. As a result, the lacZ portion of the fusion should be absent, and the *Xenopus*-produced fusion proteins should be slightly smaller than their counterparts expressed in *E. coli* (Figure 1, B and D).

Oocyte-expressed nucleolin fusion proteins were tested first for their ability to bind single-stranded DNA. Hand isolated nuclei from noninjected oocytes contain two prominent DNA-binding proteins of 90 and 95 kDa (Figure 3A, lane 1). These are the endogenous versions of *Xenopus* nucleolin that we previously characterized by this filter binding assay (DiMario and Gall, 1990). In addition to the two endogenous nucleolin proteins, hand-isolated nuclei from oocytes that were injected with mRNA encoding *myc*-tagged, full-length nucleolin (Figure 1B), contained a novel DNA-binding protein of 102 kDa. The size of the novel protein suggested that the predicted 8.7 kDa *myc* tag was fused to a protein of 93.8 kDa, which is in close agreement with the observed apparent weights of either the 90 or the 95 kDa endogenous nucleolin protein. All other detected binding proteins from the nuclei of injected oocytes were common to nuclei of noninjected oocytes (compare Figure 3A, lanes 1 and 2).

The western blot used in Figure 3A was reprobed with mAb 9E10 (Figure 3B). Nuclei from noninjected oocytes contained no detectable antigen (Figure 3B, lane 1'), whereas an antigen of 102 kDa was found in the

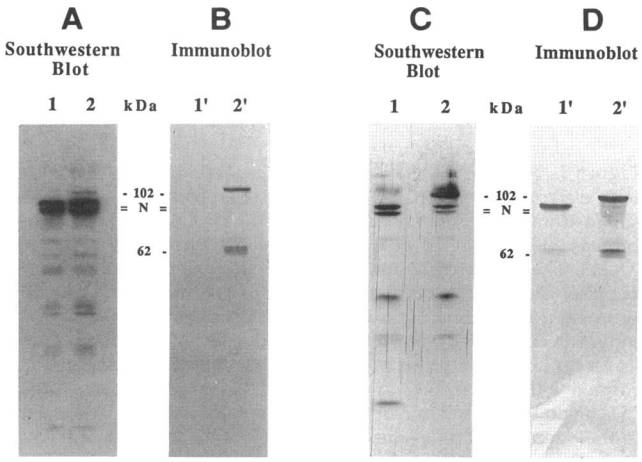

Figure 3. Western blots displayed oocyte-expressed *myc*-tagged nucleolin fusion proteins. (A) The blot was probed with single-stranded radiolabeled DNA. Nuclei from noninjected oocytes contained endogenous nucleolin proteins of 90 and 95 kDa (N), as well as minor binding proteins (lane 1). An equal number of nuclei from injected oocytes contained the endogenous nucleolin proteins and the same minor nucleic acid binding proteins found in noninjected oocytes. They also contained a novel binding protein at 102 kDa (lane 2). (B) The blot used in A was reprobed with mAb 9E10. No antigen was detected in nuclei from noninjected oocytes (lane 1'). However, the novel 102-kDa nucleic acid-binding protein and a 62-kDa antigen were labeled by mAb 9E10 (lane 2'). The 62-kDa antigen clearly contained the *myc*-tags and at least the amino terminal one-third of nucleolin. (C) A Southwestern blot characterized the GAR truncation. Nuclei from oocytes injected with mRNA transcribed from p*myc*-*Xl*C23δGAR-NO38 contained DNA-binding proteins at 90 and 95 kDa (lane 1). Nuclei from oocytes injected with mRNA transcribed from p*myc*-*Xl*C23-NO38 were used as a positive control (lane 2). (D) The blot used in C was reprobed with mAb 9E10. The *myc*-tagged GAR-truncation comigrated with the 95-kDa endogenous nucleolin.

nuclear extracts from oocytes that had been injected with the mRNA (Figure 3B, lane 2′). We concluded that the 102-kDa antigen was the epitope-tagged nucleolin fusion protein because it was found only in nuclei that were isolated from injected oocytes, and because it had an identical apparent molecular weight when compared to the novel DNA-binding protein in the Southwestern assay.

As in the *E. coli* extracts, a *myc*-tagged proteolytic fragment was found in the nuclear extracts from mRNA-injected oocytes (Figure 3B, lane 2′). Its apparent molecular weight of 62 kDa indicated that it contained, in addition to the *myc*-tags, at least the amino terminal one-third and perhaps even the first two RNA-binding domains within the carboxy terminal two-thirds of nucleolin. The similarity in size between the *E. coli*-expressed, *myc*-tagged, 64-kDa proteolytic fragment and the *myc*-tagged 62-kDa *Xenopus* fragment intrigued us. If we assume that these fragments were in fact generated from intact nucleolin by proteolysis, and if we allow for the presence of the short lacZ peptide on the 64-kDa *E. coli* fragment versus the 62-kDa oocyte fragment, then nucleolin expressed in either *E. coli* or *Xenopus* oocytes may have been cleaved at sites that lie in close proximity. Reports have suggested that proteolysis is a programmed event in the maturation of the 110-kDa CHO nucleolin (Bugler *et al.*, 1982; Bourdon *et al.*, 1983a) with the size of CHO proteolytic fragments ranging from 45–95 kDa (Bourdon *et al.*, 1983b). Chen *et al.* (1991) also suggested that human nucleolin of 105 kDa actually cleaved itself to generate several fragments ranging from 45 to 97 kDa.

In addition to the *myc*-tagged full-length protein, we also tested the oocyte-expressed GAR truncation for its ability to bind radiolabeled DNA by Southwestern assay. However, a novel DNA-binding protein was not evident (Figure 3C, lane 1). Staining the blot with mAb 9E10 showed that the tagged GAR truncation was in fact present within the nuclear extract but that it comigrated with the 95-kDa endogenous nucleolin protein (Figure 3D, lane 1′). In characterizing the oocyte-expressed GAR truncation, we concomitantly expressed full-length *myc*-tagged nucleolin in separate oocytes as a positive control for DNA binding, as a control for antibody (mAb 9E10) staining, and as a demonstration of a shift in molecular weight between the GAR truncation and the intact nucleolin fusion protein (Figure 3, C and D, lanes 2, 2′). Unfortunately, the comigration of the GAR truncation with the 95-kDa endogenous protein negated our attempts to test the in vitro binding capabilities of the GAR truncation by this one-dimensional Southwestern assay.

Because dimethylation does not change the positive charge of the arginine side group (Ghisolfi *et al.*, 1992), we reasoned that the GAR truncation should be more acidic than the endogenous proteins because of the lack of the arginine-rich domain. Therefore, a 2-D Southwestern blot was employed to separate the endogenous forms of nucleolin from the *myc*-tagged GAR truncation. The 2-D protein blot was probed with labeled DNA (Figure 4A) and then with mAb 9E10 (Figure 4B). Several isoelectric variants of the 90- and 95-kDa endogenous nucleolin proteins were evident by DNA-binding. These variants exist probably because of various degrees of nucleolin phosphorylation. The most acidic DNA-binding protein of 95 kDa (Figure 4A) colocalized with an antigen that stained well with mAb 9E10 (Figure 4B). This colocalization indicated that the oocyte-expressed *myc*-tagged GAR truncation maintained some nucleic acid binding capabilities.

Evidence from *E. coli* expression experiments showed that the smallest *myc*-tagged (i.e., mAb 9E10-positive) proteolytic fragment of ~10 kDa could be labeled by mAb G1C7. This indicated that the G1C7 epitope resided within the amino terminal region of nucleolin. With this knowledge, we used mAb G1C7 to roughly estimate the amount of the GAR truncation present within the oocyte nuclear extract relative to endogenous nucleolin proteins by comparing a combination of mAb G1C7 staining intensities and autoradiographic spot sizes on the 2-D blots. For this comparison we used another aliquot of the same protein sample used in Figure 4, A and B. On the basis of G1C7 staining (Figure 4C), we conservatively estimated that the amount of GAR truncation within the lysate was comparable to one of the minor isoelectric variants (see arrows in Figure 4C). But when the DNA-binding signals of the GAR truncation and the same isoelectric variant were compared (arrows in Figure 4A), it appeared that the GAR truncation failed to bind DNA as efficiently as did the minor isoelectric variant.

Finally, mAb G1C7 labels higher molecular weight proteins that have less acidic isoelectric points (arrowhead in Figure 4C). These proteins have not been identified, and this cross-reactivity precludes us from using mAb G1C7 in fluorescence localization experiments described below.

Characterization of Anti-Nucleolin Serum R2D2

Before we could pursue the localization of *myc*-tagged nucleolin in *Xenopus* oocyte nuclei, it was first necessary to establish the localization of endogenous nucleolin. Because mAb G1C7 labeled proteins other than nucleolin (Figure 4C), a highly specific polyclonal serum directed against *Xenopus* nucleolin was prepared. The two versions of nucleolin were purified from S100 cell extracts (Figure 5A, lane 1) of cultured *Xenopus* kidney cells by DEAE chromatography and then by poly[G] "affinity" chromatography. Nucleolin prepared by this two-step procedure was considered highly enriched by silver stain analysis (Figure 5A, lane 2), and those fractions containing only nucleolin were used for antibody production. The resulting anti-nucleolin serum, R2D2,

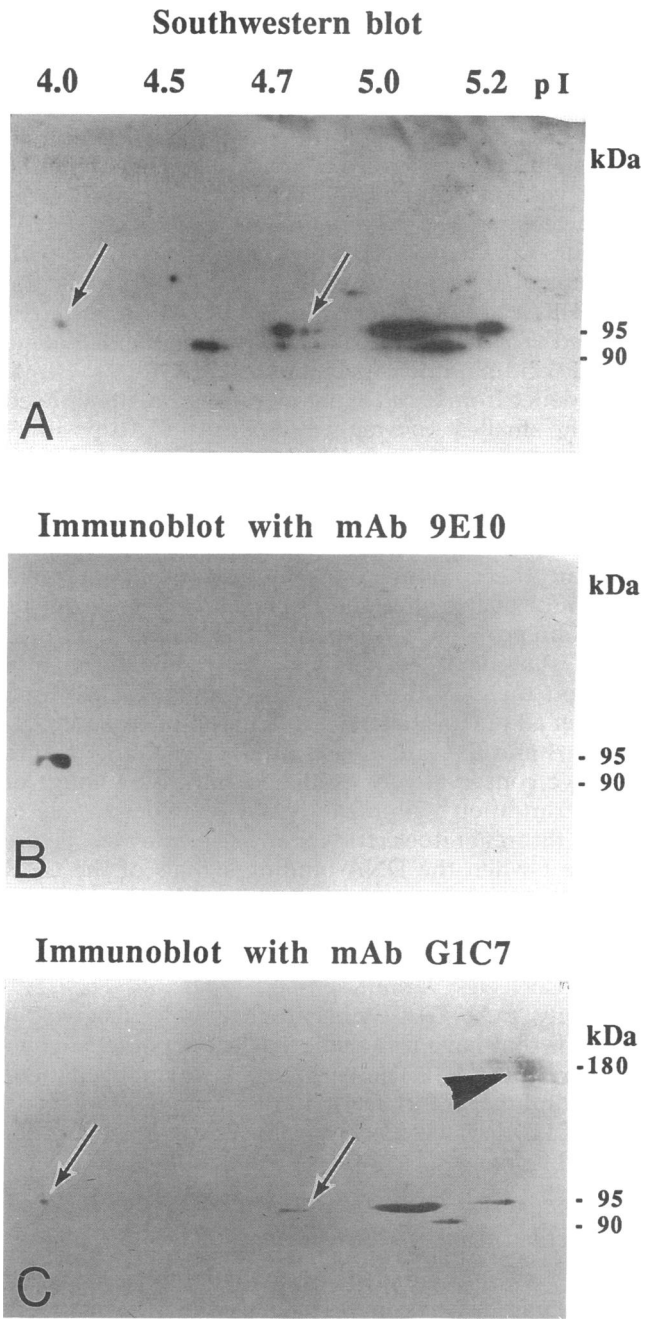

Figure 4. 2-D protein gels were used to separate the oocyte-expressed GAR truncation from endogenous nucleolin proteins. (A) The subsequent Southwestern blot showed several isoelectric variants of nucleolin at the 90 and 95 kDa range. Arrows point to the most acidic DNA-binding protein and an endogenous variant with a stronger binding signal. (B) The blot used in A was reprobed with mAb 9E10. The *myc*-tagged GAR truncation focused and comigrated with the minor nucleic acid binding protein in A. No other antigen was detected. (C) A separate blot containing proteins from the same nuclear extract as used in A and B was probed with mAb G1C7 to estimate the relative amounts of endogenous versions of nucleolin versus the GAR truncation. By staining intensity and spot size, the endogenous variant noted in (A) appeared to be underrepresented when compared to the GAR truncation.

labeled only the two nucleolin proteins versus a large complex mixture of cellular proteins (Figure 5B, lanes 1–3).

Endogenous Nucleolin Localizations

Previous reports showed that nucleolin primarily associates with the dense fibrillar regions of nucleoli (Noaillac-Depeyre *et al.* 1989; Biggiogera *et al.* 1991). Fibrillarin is a nucleolar-specific protein that is known to reside within the dense fibrillar regions (Ochs *et al.*, 1985). Therefore, to identify the dense fibrillar regions of the multiple nucleoli, we prepared the contents of nuclei from noninjected oocytes according to the procedures of Gall *et al.* (1991), and then probed these preparations with mouse anti-fibrillarin antibody, mAb 72B9, followed by fluorescein-coupled goat anti-mouse. Figure 6A is a phase contrast micrograph showing several *Xenopus* oocyte nucleoli that were prepared from the same nucleus but ranged in size from 5 to 10 μm. mAb 72B9 staining was restricted to internal regions (dense fibrillar regions) of the nucleoli, whereas the peripheral regions (the granular regions) were not stained. No other nuclear structure was stained by mAb 72B9 (Figure 6B). We next counterstained these same nucleoli with rabbit serum R2D2 and rhodamine-coupled mouse anti-rabbit (Figure 6C). R2D2 intensely stained the same regions that mAb 72B9 stained. The colocalization of mAb 72B9 and our rabbit anti-nucleolin clearly established that fibrillarin and nucleolin colocalized to the dense fibrillar regions of the multiple nucleoli. Besides the dense fibrillar regions, however, R2D2 also lightly stained the surrounding granular regions of the nucleoli; the presence of nucleolin within nucleolar granular regions has been previously described (Noaillac-Depeyre *et al.* 1989; Biggiogera *et al.* 1991). The staining patterns in Figure 6, B and C indicated that the granular regions of these *Xenopus* multiple nucleoli were very narrow bands surrounding the dense fibrillar regions and that the granular regions constituted a small percentage of the overall nucleolar mass.

We often observed understained spots within the very center of the nucleoli with either mAb 72B9 (Figure 6B) or R2D2 (Figure 6C). We interpreted these regions as the fibrillar centers that were noted to be deficient in fibrillarin (Ochs *et al.*, 1985) and nucleolin (Noaillac-Depeyre *et al.*, 1989; Biggiogera *et al.*, 1991) by antibody staining.

Anti-nucleolin serum R2D2 also lightly stained the RNP material surrounding the nucleoli (Figure 6C). This staining was not simply background fluorescence, because nuclear preparations probed only with the rhodamine-coupled secondary antibody showed no staining of this RNP material. Recall that the R2D2 serum detected only nucleolin on the Western blots (Figure 5D), and this specificity of R2D2 suggested that nucleolin may be more widely distributed throughout the

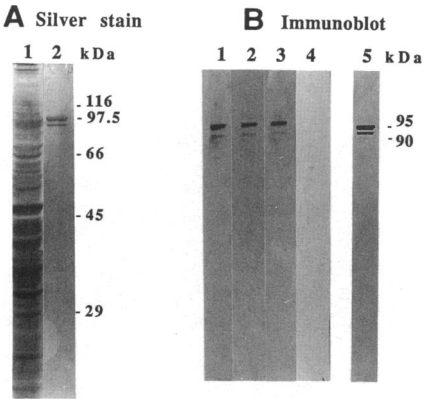

Figure 5. Purification of *Xenopus* nucleolin and the characterization of rabbit anti-*Xenopus* nucleolin serum, R2D2. Nucleolin was purified from S100 extracts of *Xenopus* kidney cells by DEAE and poly[G] chromatography. (A) Silver-stained SDS 10% polyacrylamide gels show the complex protein mixture from which nucleolin was purified (lane 1). Final poly[G] fractions were considered highly enriched for nucleolin by silver stain analysis (lane 2). (B) Fractions enriched for nucleolin were used to produce polyclonal rabbit serum R2D2. The complex protein mixture as in A (lane 1) was blotted and probed with R2D2 diluted 1/200 (lane 1), 1/500 (lane 2), and 1/1000 (lane 3). R2D2 labeled only nucleolin in the mixture. The preimmune rabbit serum was tested at 1/100 (lane 4). Enriched nucleolin as in A (lane 2) was blotted and probed with R2D2 (lane 5).

nucleus rather than localized solely to the nucleoli (Rankin and DiMario, unpublished data).

Nucleolar Localizations of myc-Tagged Nucleolin Fusion Proteins

Ultimately, we hope to use tagged nucleolin to characterize nucleolar structure and function in vivo, and nucleolar localization should be the first prerequisite in determining whether or not *myc*-tagged wild-type nucleolin can function properly in vivo. The results of Figure 3 indicated that tagged wild-type nucleolin translocated into the nuclei. To determine its location within the nuclei, we again injected stages 5 and 6 *Xenopus* oocytes with mRNA synthesized in vitro from p*myc*-*Xl*C23-NO38. The oocytes were cultured for 18–24 h at 18°C to allow *myc*-tagged nucleolin synthesis and translocation into the nuclei. The nuclear contents were then prepared for immunofluorescence microscopy. This oocyte product is depicted in Figure 1B.

Localization of *myc*-tagged full-length nucleolin to the nucleoli by staining with mAb 9E10 and fluorescein-coupled goat anti-mouse is shown in Figure 7B. In addition to the nucleoli, surrounding RNP particles were stained, which indicated that the *myc*-tagged nucleolin associated with these extranucleolar RNP particles, as Figure 6C indicated. We assume that part of this extranucleolar staining was because of an overexpression of the fusion protein and that the majority of tagged nucleolin was actually not associated with the multiple nucleoli. The immunoblots of Figure 3 showed that the majority of *myc*-tagged nucleolin was intact. This suggested that the immunofluorescence staining in Figure 7B also localized mostly intact nucleolin fusion protein.

Besides labeling endogenous nucleolin, mouse mAb G1C7 (Figure 4C) and rabbit serum R2D2 label *myc*-tagged versions of nucleolin on Western blots. Therefore, we cannot localize only endogenous nucleolin versus *myc*-tagged nucleolin by using either antibody. However, if *myc*-tagged nucleolin colocalized with endogenous versions of nucleolin, the staining patterns with mouse mAb 9E10 and rabbit serum R2D2 should be similar. To test this we counterstained the nucleoli of Figure 7A with R2D2 and rhodamine-coupled goat anti-rabbit IgG. Figure 7C shows similar staining patterns as in Figure 7B. The colocalization of *myc*-tagged full-length nucleolin with endogenous nucleolin indicated that the *myc* tags did not interfere with nuclear translocation nor with nucleolar association.

In most cases, staining with the anti-nucleolin serum was very bright, and substructure was not readily discernable. However, some of the larger nucleoli that were separated away from the RNP material showed detailed substructure when stained with 9E10 or R2D2. The top left insets in Figure 7, A–C show such nucleoli from a similarly injected oocyte. Both mAb 9E10 and R2D2 stained the phase-dense regions of these nucleoli. Based upon the localizations of Figure 7, A–C, we concluded that the *myc*-tagged, full-length nucleolin colocalized with endogenous nucleolin primarily within the dense fibrillar regions of the nucleoli that were defined by the double-labeling experiment of Figure 6.

In the above double-labeling experiments, we first probed the nuclear preparations with mAb 9E10 and fluorescein-coupled goat anti-mouse antibody. We recorded the fluorescein results on film before reprobing with R2D2 and rhodamine-coupled mouse anti-rabbit. The reason for this laborious approach was to eliminate the possibility that fluorescein-coupled goat anti-mouse antibody might cross-react with R2D2 or the rhodamine-coupled mouse anti-rabbit. To control for the possibility that the rhodamine-coupled mouse anti-rabbit IgG cross-reacted with mAb 9E10 or the fluorescein-coupled goat anti-mouse used to detect mAb 9E10, we probed the nuclear contents from a similarly injected oocyte (Figure 7A, top right inset) with mAb 9E10 and fluorescein-coupled goat anti-mouse. We left out rabbit serum R2D2 but reprobed with rhodamine-coupled mouse anti-rabbit. A strong signal was again detected in the fluorescein channel that localized *myc*-tagged nucleolin to the nucleoli (Figure 7B, top right inset), but no signal was detected in the rhodamine channel (Figure 7C, top right inset). This control was necessary to show that cross-reactivity by rhodamine-coupled mouse anti-rabbit with mAb 9E10 or its fluorescein-coupled secondary antibody did not account for the signals in Figure 7C.

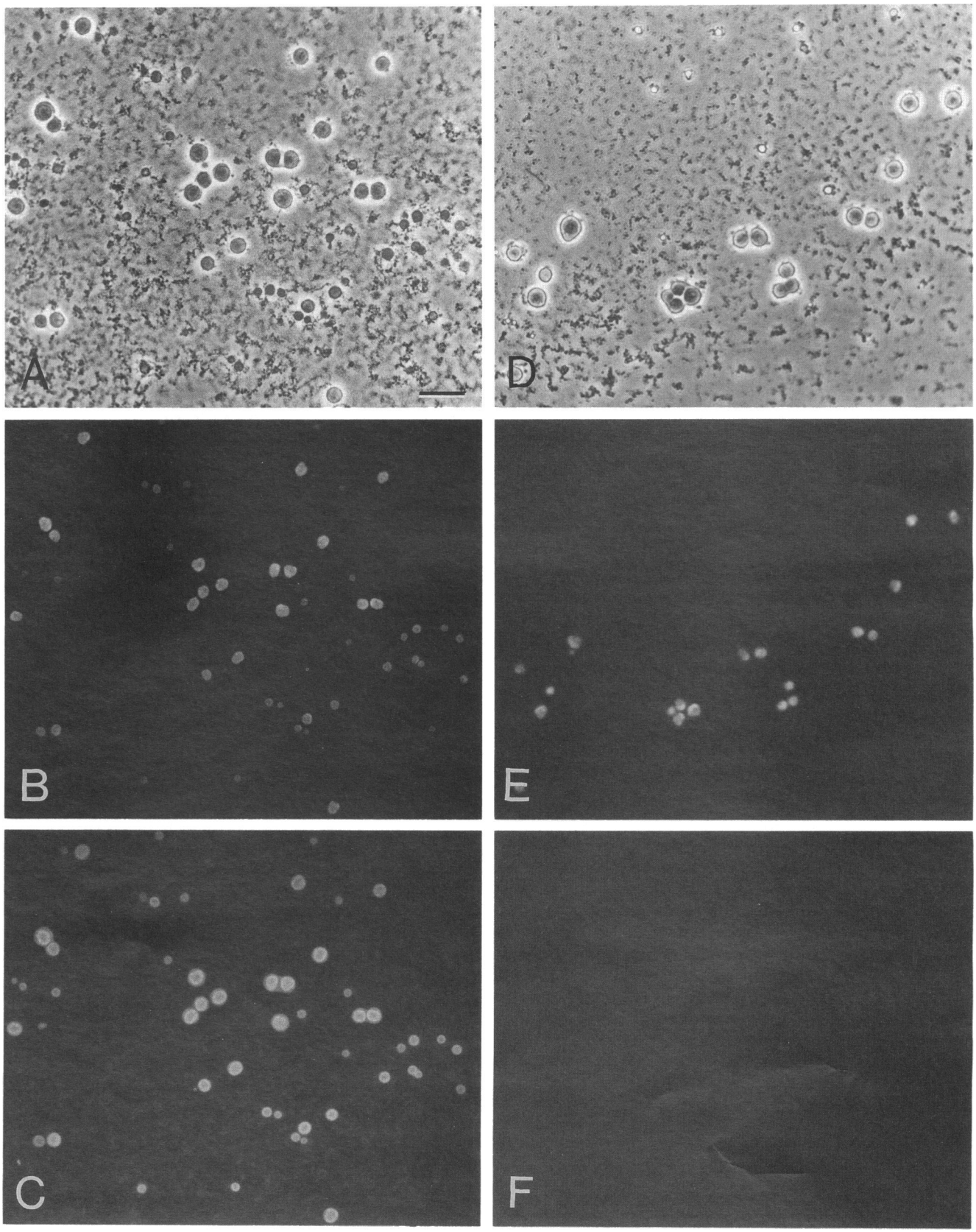
A
D
B
E
C
F

The GAR Truncation Failed to Efficiently Associate with the Multiple Nucleoli

The GAR-truncated protein expressed in *E. coli* completely failed to bind nucleic acid as compared to the full-length *E. coli* fusion protein. In addition, whereas the full length fusion expressed in *Xenopus* oocytes readily bound nucleic acids, the GAR truncation expressed in oocytes appeared to have reduced binding activities when compared to an endogenous isoelectric variant of comparable abundance within oocyte nuclei (Figure 4). Its reduced in vitro nucleic acid binding capabilities next prompted us to determine if the GAR truncation could properly associate with nucleoli in vivo.

We knew from the results of Figure 3D and Figure 4 that the *myc*-tagged GAR truncation successfully translocated from the site of synthesis in the cytoplasm into the nuclei. To determine if the GAR-truncation associated with the multiple nucleoli, oocytes were again injected with mRNA that was in vitro transcribed from p*myc*-*Xl*C23δGAR. The oocyte translation product is depicted in Figure 1D. When probed with mAb 9E10, the multiple nucleoli were reproducibly understained (Figure 7E) as compared to nucleoli from oocytes that were injected with mRNA encoding *myc*-tagged full-length nucleolin (e.g., see Figure 7, B and E).

As with the localization of *myc*-tagged full-length nucleolin, the tagged GAR truncation associated with extranucleolar RNP material. On the basis of similar RNP staining intensities in Figure 7, B and E, the amount of tagged GAR truncation within the extranucleolar RNP material appeared comparable to the amount of tagged full-length nucleolin within this material. In the absence of any significant nucleolar staining in Figure 7E, this RNP staining served as an internal positive control for the presence of the GAR truncation within the nuclei, as Figure 3D indicated.

Anti-nucleolin rabbit serum R2D2 was again used to localize both the endogenous nucleolin and the GAR-truncation. R2D2 stained the nucleoli that demonstrated the presence of only endogenous nucleolin (Figure 7F) and, as expected, R2D2 stained the extranucleolar RNP material. The differential nucleolar staining with mAb 9E10 versus R2D2 (e.g., compare Figures 7, E and F) clearly demonstrated that the *myc*-tagged GAR truncation failed to efficiently localize to the multiple nucleoli.

Finally, to control for the possibility that the fluorescein-coupled goat anti-mouse cross-reacted with the RNP material and for autofluorescence in the fluorescein channel, a similar preparation from an injected oocyte (Figure 7D inset) was probed with only this secondary antibody and not mAb 9E10. No signal was detected (Figure 7E inset).

DISCUSSION

We have chosen the *Xenopus* oocyte to gain more information about the in vivo associations of nucleolin. Ribosomal DNA amplifies in the pachytene stage of oogenesis by rolling circle replication (Brown and Dawid, 1968; Gall, 1968). As much as 30 pg of rDNA per oocyte is then separated into multiple nucleoli; the nucleus of a typical diplotene *Xenopus* oocyte contains ~1000 extra-chromosomal nucleoli. Transcription of this rDNA produces large quantities of nascent 45S ribosomal RNA that is quickly processed to yield mature 18S, 5.8S, and 28S ribosomal RNA (reviewed by Gerbi *et al.*, 1990). The production of ribosomes in the diplotene oocyte is tremendous; some 300 000 ribosomes are assembled per second within the oocyte (Scheer, 1973), whereas 10–100 ribosomes are assembled per second in a typical nondividing somatic cell (Hadjiolov, 1985). Besides the high rates of ribosome production, other advantages in using *Xenopus* oocytes to study nucleolin are first, nucleolin is abundant in *Xenopus* oocytes (DiMario and Gall, 1990), and second, the amplified nucleoli can be prepared for light microscopy such that their structural integrity is well preserved (Callan *et al.*, 1987). These amenities should allow us to study the localization of epitope-tagged wild-type and mutagenized forms of nucleolin by injecting their respective in vitro synthesized mRNAs into *Xenopus* oocytes. Localization of mutagenized forms of nucleolin should identify what domains are important for nucleolar associations.

The ability of nucleolin to bind both RNA and DNA in vitro has been well documented (Olson *et al.*, 1983; Bugler *et al.*, 1987; Sapp *et al.*, 1989; DiMario and Gall, 1990; Barrijal *et al.*, 1992). We have shown that epitope-tagged full-length nucleolin expressed in *E. coli* or in *Xenopus* oocytes maintains the ability to nonspecifically bind radiolabeled nucleic acids (e.g., DNA) in vitro. However, large proteolytic nucleolin fragments found in *E. coli* extracts that lacked short regions of their carboxy termini failed to bind radiolabeled DNA. These proteolytic truncations suggested that the GAR domain may be important for this observed in vitro nucleic acid

Figure 6. Double-labeling localized endogenous fibrillarin and nucleolin within the dense fibrillar regions of *Xenopus* oocyte nucleoli. Micrographs A and D are phase contrast images of the nuclear contents from noninjected oocytes. Micrographs B, C, E, and F are fluorescent images. (B) The nuclear preparation shown in A was probed with mouse anti-fibrillarin mAb 72B9 and fluorescein-coupled goat anti-mouse IgG. The fluorescein results were recorded on film first. (C) The preparation was reprobed with rabbit anti-nucleolin R2D2 and rhodamine-coupled mouse anti-rabbit IgG. Both antibodies stained the nucleoli showing a colocalization of fibrillarin and nucleolin. (E) The nuclear preparation in D was probed with mAb 72B9 and fluorescein-coupled goat anti-mouse as in B. (F) The preparation was reprobed only with rhodamine-coupled mouse anti-rabbit. Rabbit serum R2D2 was not used. E and F controlled for possible cross-reactivity of the rhodamine-coupled mouse anti-rabbit with either mAb 72B9 or the fluorescein-coupled goat anti-mouse IgG. Bar, 20 μm.

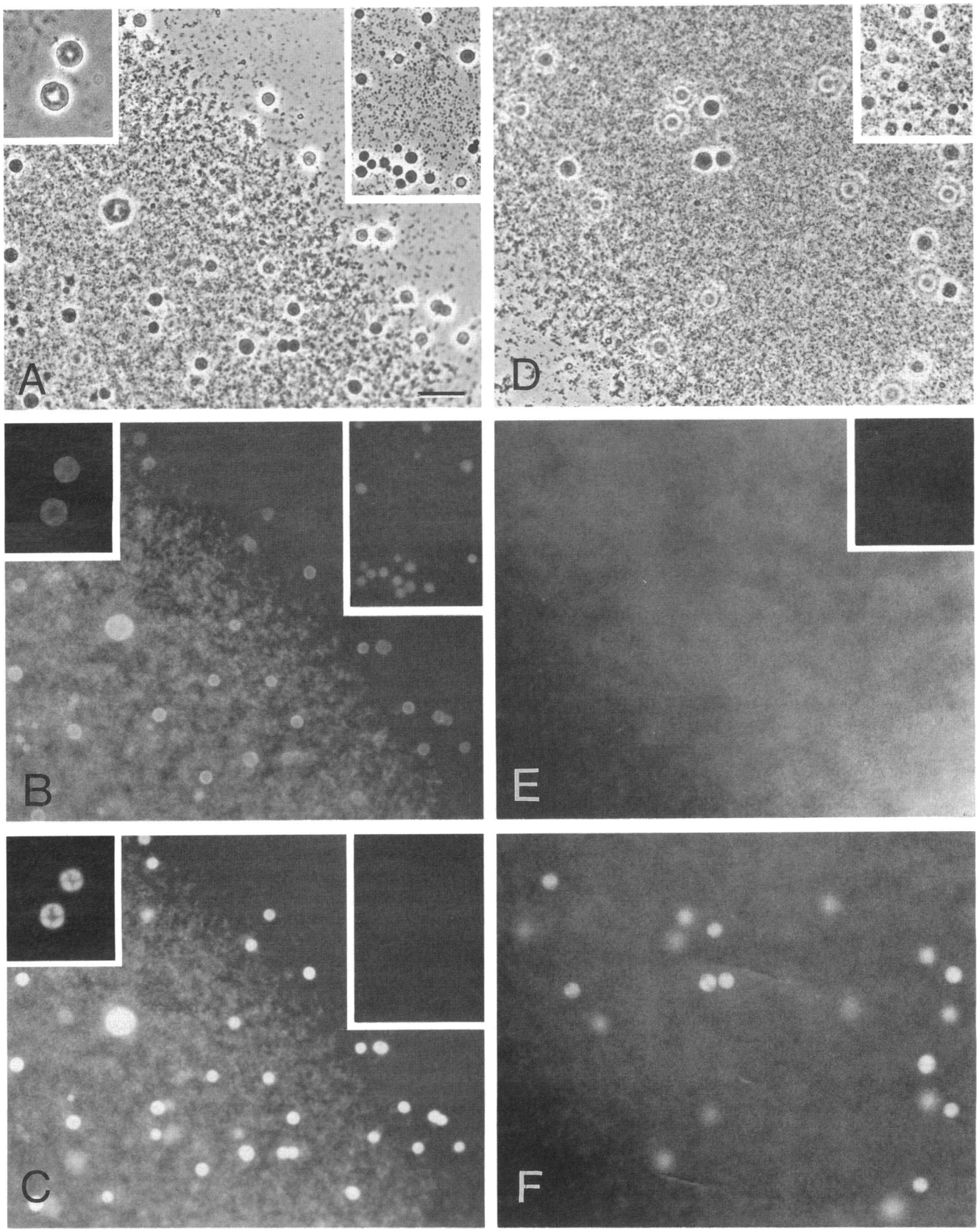
A
D
B
E
C
F

binding activity. To specifically address this possibility, we truncated nucleolin by introducing a stop codon shortly before the GAR domain. *E. coli*-expressed fusion proteins truncated in this manner completely failed to bind radiolabeled probes as compared to the full-length *E. coli* fusion protein. This indicates that the GAR domain is important for in vitro nucleic acid binding.

The GAR-truncation expressed in *Xenopus* oocytes maintains some detectable binding activity. Specific posttranslational modifications such as phosphorylation within the amino terminal third of nucleolin (Ballal *et al.*, 1975; Geahlen and Harrison, 1984; Belenguer *et al.*, 1990; Peter *et al.*, 1990) may explain why the *Xenopus*-produced GAR truncation maintains some binding activity versus the *E. coli*-produced GAR truncation. A direct comparison of the *Xenopus* GAR truncation and the *E. coli* GAR truncation may not be appropriate because of uncertainties in posttranslational modifications of the two proteins. However, we note that the in vitro binding efficiency of the oocyte-expressed GAR truncation appears to be less than that of an endogenous full-length isoelectric variant of similar (probably less) abundance (Figure 4, A and C). This observation suggests that the GAR domain may be required for at least efficient nucleic acid binding by intact nucleolin.

Ghisolfi *et al.* (1992) showed that on its own, the GAR domain can bind nucleic acids in vitro with a dissociation constant of $0.5 \times 10^6\ M^{-1}$. In support of our findings, they also showed that the association of the GAR domain with nucleic acid was not as tight as that observed for intact nucleolin that had a dissociation constant of $2 \times 10^7\ M^{-1}$. The difference in dissociation constants between the GAR domain on its own versus intact nucleolin suggests that intramolecular interactions occur between the GAR domain and the rest of the protein to enhance nucleic acid binding.

Such intramolecular interactions have been previously suggested for proper nucleolin function. For example, Sapp *et al.* (1989) described a sixfold higher renaturation rate for heat-denatured DNA restriction fragments in the presence of intact nucleolin as compared to the renaturation rate observed for just the 48-kDa carboxy two-thirds of nucleolin. Their results suggested that an interaction between the amino terminal third and the carboxy terminal two-thirds facilitates single-strand DNA renaturation. Second, Olson *et al.* (1990) showed a substantial increase in chymotrypsin sensitivity within the amino terminal third when intact nucleolin was incubated in the presence of poly[G] versus in the absence of poly[G]. Because the four RNA-binding domains were chiefly responsible for binding poly[G], these latter results indicated that a conformational change takes place within the amino terminal third of nucleolin when the protein's carboxy two-thirds binds nucleic acid.

We have used radiolabeled single-stranded DNA in our Southwestern assays mostly to monitor the presence and nucleic acid binding capabilities of nucleolin under defined in vitro conditions. Although specific in vitro nucleolin-DNA interactions have been noted (Barrijal *et al.*, 1992), we stress that our Southwestern assays should not be interpreted to reflect in vivo function. The demonstration that the GAR domain is important for nucleic acid interaction in our filter binding assays, however, suggests that it may also play an important role in the proper in vivo association with nucleic acids in the nucleoli. Therefore, in an attempt to study nucleolin's in vivo associations, we expressed epitope-tagged full-length and GAR-truncated nucleolin in *Xenopus* oocytes.

Immunofluorescence results showed that full-length *myc*-tagged nucleolin properly translocates to the nuclei and then associates with nucleoli despite the tags on the amino terminal end and the presence of endogenous nucleolin within the nucleoli. This proper localization suggests that the full-length fusion protein has the potential to function normally in vivo. Previous nucleolar localization studies by Peculis and Gall (1992) showed that *Xenopus* nucleolar protein, NO38, properly localizes to oocyte nucleoli when a single *myc* epitope was used as the tag.

The full length *myc*-tagged nucleolin also localized to extranucleolar RNP particles. This simply may be a result of an overexpression of fusion protein within the oocytes. However, our rabbit anti-nucleolin serum, R2D2, also labeled extranucleolar RNP particles within the nuclei of noninjected oocytes (Figure 6C). This extranucleolar nucleolin may be involved either in shuttling (Borer *et al.*, 1989) or perhaps in the processing of RNAs other than ribosomal RNA. The *myc*-tagged GAR

Figure 7. Double-labeling experiments localized *myc*-tagged full length and GAR-truncated nucleolin versus endogenous nucleolin. A and D are phase contrast micrographs of nuclear preparations made from oocytes that had been injected with mRNA encoding *myc*-tagged full-length nucleolin (A) or the *myc*-tagged GAR truncation (D). (B) The preparation in A was stained with mAb 9E10 and fluorescein-coupled goat anti-mouse IgG to detect the *myc*-tagged full-length nucleolin fusion protein. The multiple nucleoli and the surrounding RNP material stained. (C) The preparation in A was reprobed with rabbit anti-nucleolin serum, R2D2, and rhodamine-coupled mouse anti-rabbit IgG to localize endogenous and tagged nucleolin. Similar staining patterns in B and C indicated that the *myc*-tagged fusion properly localized to the nucleoli. As a control for cross-reactivity, a similar preparation (A, top right inset) was probed mAb 9E10 and fluorescein-coupled goat anti-mouse (B, top right inset) and then with only the rhodamine-coupled secondary antibody, not R2D2 (C, top right inset). No staining was observed in the rhodamine channel. (E) The preparation in D was probed with mAb 9E10 and the fluorescein-coupled anti-mouse IgG. The multiple nucleoli were not stained above the surrounding RNP material. (F) The preparation in G was reprobed with anti-nucleolin serum, R2D2; the nucleoli were brightly stained above the surrounding RNP material. Bar, 20 μm.

truncation also localized to the extranucleolar RNP material (Figure 7H), perhaps by interactions with its four intact RNA-binding domains. Further investigations into the extranucleolar localization of nucleolin within amphibian oocyte nuclei are underway (Rankin and DiMario, unpublished data).

Our *myc*-tagged nucleolin GAR truncation failed to efficiently localize to the multiple nucleoli despite its translocation into the nuclei and its accumulation within the extranucleolar RNP material (Figure 7H). Failure of the GAR truncation to specifically associate with nucleoli may be because of an absence of direct interactions that normally occur between the GAR domain and nucleolar macromolecules such as rRNA, or perhaps other nucleolar proteins. Alternatively, various other nucleolin domains such as the four RNA-binding domains or the alternating basic and acidic regions may fail to properly interact with nucleolar macromolecules because of improper tertiary configurations that normally occur when the GAR domain is present.

Other proteins that contain GAR-like domains include fibrillarin (referred to as NOP1 in yeast) that associates with nucleolar U3 snRNA and plays a positive role in pre-rRNA processing (Kass *et al.*, 1990), the yeast nucleolar protein GAR 1 that is essential for pre-rRNA processing (Girard *et al.*, 1992), the yeast nucleolar protein SSB-1 (Jong *et al.*, 1987) that associates with small nuclear RNAs snR10 and snR11 (Clark *et al.*, 1990), NSR1 that is the yeast analogue of vertebrate nucleolin (Kondo *et al.*, 1992a,b), and the vertebrate hnRNP proteins A1 and U (Dreyfuss *et al.*, 1993). In addition, the protein product of the fragile X gene, *FMR1*, has recently been shown to contain a GAR domain (referred to as the RGG box by Siomi *et al.*, 1993). The FMR1 protein binds RNA in vitro, and deletion of its GAR domain removes the capacity of this protein to bind RNA in vitro (Siomi *et al.*, 1993). We have shown that the GAR domain of nucleolin is also necessary for in vitro nucleic acid binding and specific localization of nucleolin within nucleoli. We are currently testing whether nucleolin's GAR domain can confer RNA-binding and nucleolar localization characteristics on non-RNA-binding, nonnucleolar proteins.

ACKNOWLEDGMENTS

We thank Monique LeBlanc and Karen Jones for technical assistance on portions of this research. We also thank Dr. Mark Roth for the Myc-6D construct and for the hybridoma cell line producing mAb G1C7. This work was separately supported by grants from the Louisiana Education Quality Support Fund [LEQSF (1992–95)-RD-A-04] and the National Science Foundation (MCB-9204769).

Note added in proof. After resubmitting our revised manuscript, Schmidt-Zachmann *et al.* (1993, Cell 74, 493–504) showed that chicken nucleolin that had been truncated for its GAR domain failed to localize to nucleoli in human-mouse heterokaryons. Schmidt-Zachmann and Nigg (1993, J. Cell Sci. *105*, 799–806) further showed that when nucleolin's GAR domain was attached to cytoplasmic pyruvate kinase, the fusion did not localize to nucleoli. This latter result suggests that by itself, the GAR domain does not act as a nucleolar localization signal.

REFERENCES

Ballal, N.R., Kang, Y., Olson, M.O.J., and Busch, H. (1975). Changes in nucleolar proteins and their phosphorylation patterns during liver regeneration. J. Biol. Chem. *250*, 5921–5925.

Barrijal, S., Manoussos, P., Gu, Z., Avalosse, B.L., Belenguer, P., Amalric, F., and Rommelaere, J. (1992). Nucleolin forms a specific complex with a fragment of the viral (minus) strand of minute virus of mice DNA. Nucleic Acids Res. *20*, 5053–5060.

Belenguer, P., Caizergues-Ferrer, M., Labbe, J., Doree, M., and Amalric, F. (1990). Mitosis-specific phosphorylation of nucleolin by $p34^{cdc2}$ protein kinase. Mol. Cell. Biol. *10*, 3607–3618.

Biggiogera, M., Kaufmann, S.H., Shaper, J.H., Gas, N., Amalric, F., and Fakan, S. (1991). Distribution of nucleolar proteins B23 and nucleolin during mouse spermatogenesis. Chromosoma *100*, 162–172.

Borer, R.A., Lehner, C.F., Eppenberger, H.M., and Nigg, E.A. (1989). Major nucleolar proteins shuttle between nucleus and cytoplasm. Cell *10*, 379–390.

Bourdon, H.M., Bugler, B., Caizergues-Ferrer, M., and Amalric, F. (1983a). Role of phosphorylation on the maturation pathways of a 100 kDa nucleolar protein. FEBS Lett. *155*, 218–222.

Bourdon, H.M., Bugler, B., Caizergues-Ferrer, M., Amalric, F., and Zalta, J.P. (1983b). Maturation of a 100 kDa protein associated with preribosomes in Chinese hamster ovary cells. Mol. Biol. Rep. *9*, 39–47.

Brinkmann, U., Mattes, R.E., and Buckel, P. (1989). High-level expression of recombinant genes in *Eschericia coli* is dependent on the availability of the *dnaY* gene product. Gene *85*, 109–114.

Brown, D.D., and Dawid, I.B. (1968). Specific gene amplification in oocytes. Science *160*, 272–280.

Bugler, B., Bourbon, H., Lapeyre, B., Wallace, M.O., Chang, J., Amalric, F., and Olson, M.O.J. (1987). RNA binding fragments from nucleolin contain the ribonucleoprotein consensus sequence. J. Biol. Chem. *262*, 10922–10925.

Bugler, B., Caizergues-Ferrer, M., Bouche, G., Bourbon, H., and Amalric, F. (1982). Detection and localization of a class of proteins immunologically related to a 100-kDa nucleolar protein. Eur. J. Biochem. *128*, 475–480.

Caizergues-Ferrer, M., Mariottini, P., Curie, C., Lapeyre, B., Gas, N., Amalric, F., and Amaldi, F. (1989). Nucleolin from *Xenopus laevis:* cDNA cloning and expression during development. Genes & Dev. *3*, 324–333.

Callan, H.G., Gall, J.G., and Berg, C.A. (1987). The lampbrush chromosomes of *Xenopus laevis:* preparation, identification, and distribution of 5S DNA sequences. Chromosoma *95*, 236–250.

Chen, C., Chiang, S., and Yeh, N. (1991). Increased stability of nucleolin in proliferating cells by inhibition of its self-cleaving activity. J. Biol. Chem. *266*, 7754–7758.

Devereux, J., Haeberli, P., and Smithies, O. (1984). A comprehensive set of sequence analysis programs for the VAX. Nucleic Acids Res. *12*, 387–395.

DiMario, P.J., Bromley, S.E., and Gall, J.G. (1989). DNA-binding proteins on lampbrush chromosome loops. Chromosoma *97*, 413–420.

DiMario, P.J., and Gall, J.G. (1990). Nucleolin from the multiple nucleoli of amphibian oocyte nuclei. Chromosoma *99*, 87–94.

Dingwall, C., Dilworth, S.M., Black, S.J., Kearsey, S.E., Cox, L.S., and Laskey, R.A. (1987). Nucleoplasmin cDNA sequence reveals polyglu-

tamic acid tracts and a cluster of sequences homologous to putative nuclear localization signals. EMBO J. *6*, 69–74.

Dreyfuss, G., Matunis, M.J., Pinol-Roma, S., and Burd, C.G. (1993). hnRNP proteins and the biogenesis of mRNA. Annu. Rev. Biochem. *62*, 289–321.

Epstein, L.M., Mahon, K.A., and Gall, J.G. (1986). Transcription of a satellite DNA in the newt. J. Cell Biol. *103*, 1137–1144.

Erard, M., Belenguer, P., Caizergues-Ferrer, M., Pantaloni, A., and Amalric, F. (1988). A major nucleolar protein, nucleolin, induces chromatin decondensation by binding to histone H1. Eur. J. Biochem. *175*, 525–530.

Erard, M., Lakhdar-Ghazal, F., and Amalric, F. (1990). Repeat peptide motifs which contain β-turns and modulate DNA condensation in chromatin. Eur. J. Biochem. *191*, 19–26.

Escande, M.L., Gas, N., and Stevens, B.J. (1985). Immunolocalization of the 100 K nucleolar protein in CHO cells. Biol. Cell *53*, 99–110.

Evan, G.I., Lewis, G.K., Ramsey, G., and Bishop, J.M. (1985). Isolation of monoclonal antibodies specific for human c-*myc* proto-oncogene product. Mol. Cell. Biol. *5*, 3610–3616.

Frohman, M.A., Dush, M.K., and Martin, G.R. (1988). Rapid production of full-length cDNAs from rare transcripts: amplification using a single gene-specific oligonucleotide primer. Proc. Natl. Acad. Sci. USA *85*, 8998–9002.

Gall, J.G. (1968). Differential synthesis of the genes for ribosomal RNA during amphibian oogenesis. Proc. Natl. Acad. Sci. USA *60*, 553–560.

Gall, J.G., Murphy, C., Callan, H.G., and Wu, Z. (1991). Lampbrush chromosomes. Methods Cell Biol. *36*, 149–166.

Geahlen, R.L., and Harrison, M.L. (1984). Induction of a substrate for casein kinase II during lymphocyte mitogenesis. Biochim. Biophys. Acta *804*, 169–175.

Gerbi, S.A., Savino, R., Stebbins-Boaz, B., Jeppesen, C., and Rivera-Leon, R. (1990). A role for U3 in the nucleolus. In: The Ribosome: Structure, Function and Evolution, ed. W. Hill, P. Moore, D. Schlessinger, A. Dahlberg, J. Warner, and R. Garrett, Washington, DC: American Society for Microbiology, 452–469.

Ghisolfi, L., Gerard, J., Amalric, F., and Erard, M. (1992). The glycine-rich domain of nucleolin has an unusual supersecondary structure responsible for its RNA-helix-destabilizing properties. J. Biol. Chem. *267*, 2955–2959.

Girard, J-P., Lehtonen, H., Caizergues-Ferrer, M., Amalric, F., Tollervey, D., and Lapeyre, B. (1992). GAR1 is an essential small nucleolar RNP protein required for pre-rRNA processing in yeast. EMBO J. *11*, 673–682.

Hadjiolov, A.A. (1985). The Nucleolus and Ribosome Biogenesis, New York: Springer-Verlag.

Herrera, A.H., and Olson, M.O.J. (1986). Association of protein C23 with rapidly labeled nucleolar RNA. Biochemistry *25*, 6258–6264.

Jong, A.Y.S., Clark, M.W., Gilbert, M., Oheim, A., and Campbell, J.L. (1987). *Saccharomyces cerevisiae* SSB1 protein and its relationship to nucleolar RNA-binding proteins. Mol. Cell. Biol. *7*, 2947–2955.

Kass, S., Tyc, K., Steitz, J.A., and Sollner-Webb, B. (1990). The U3 small nucleolar ribonucleoprotein functions in the first step of preribosomal RNA processing. Cell *60*, 897–908.

Kingston, R.E. (1993). Unit 4.5. In: Current Protocols in Molecular Biology, ed. F.M. Ausubel, R. Brent, R.E. Kingston, D.D. Moore, J.G. Seidman, J.A. Smith, and K. Struhl, New York: John Wiley and Sons.

Kondo, K., and Inouye, M. (1992a). Yeast NSR1 protein that has structural similarity to mammalian nucleolin is involved in pre-rRNA processing. J. Biol. Chem. *267*, 16252–16258.

Kondo, K., Kowalski, L.R.Z., and Inouye, M. (1992b). Cold shock induction of yeast NSR1 protein and its role in pre-rRNA processing. J. Biol. Chem. *267*, 16259–16265.

Kozak, M. (1987). At least six nucleotides preceding the AUG initiator codon enhance translation in mammalian cells. J. Mol. Biol. *196*, 947–950.

Laemmli, U.K. (1970). Cleavage of structural proteins during the assembly of the head of bacteriophage T4. Nature *227*, 680–685.

Lapeyre, B., Amalric, F., Ghaffari, S.H., Venkatarama Rao, S.V., Dumbar, T.S., and Olson, M.O.J. (1986). Protein and cDNA sequence of a glycine-rich, dimethylarginine-containing region located near the carboxy-terminal end of nucleolin (C23 and 100 kDa). J. Biol. Chem. *261*, 9167–9173.

Lapeyre, B., Bourbon, H., and Amalric, F. (1987). Nucleolin, the major nucleolar protein of growing eukaryotic cells: an unusual protein structure revealed by nucleotide sequence. Proc. Natl. Acad. Sci. USA *84*, 1472–1476.

Lischwe, M.A., Cook, R.G., Ahn, Y.S., Yeoman, L.C., and Busch, H. (1985). Clustering of glycine and N^G,N^G-dimethylarginine in nucleolar protein C23. Biochemistry *24*, 6025–6028.

Maridor, G., and Nigg, E.A. (1990). cDNA sequences of chicken nucleolin/C23 and NO38/B23, two major nucleolar proteins. Nucleic Acids Res. *18*, 128.

McStay, B., and Reeder, R.H. (1986). A terminal site for *Xenopus* RNA polymerase I also acts as an element of an adjacent promoter. Cell *47*, 913–920.

McStay, B., and Reeder, R.H. (1990). An RNA polymerase I termination site can stimulate the adjacent ribosomal gene promoter by two distinct mechanisms in *Xenopus laevis*. Genes & Dev. *4*, 1240–1252.

Monro, S., and Pelham, H.R.B. (1986). An hsp70-like protein in the ER: identity with the 78 kd glucose-regulated protein and immunoglobulin heavy chain binding protein. Cell *46*, 291–300.

Monro, S., and Pelham, H.R.B. (1987). A C-terminal signal prevents secretion of luminal ER proteins. Cell *48*, 899–907.

Nagai, K., Oubridge, C., Jessen, T.H., Li, J., and Evans, P.R. (1990). Crystal structure of the RNA-binding domain of the U1 small nuclear ribonucleoprotein A. Nature *348*, 515–520.

Noaillac-Depeyre, J., Dupont, M., Tichadou, J., and Gas, N. (1989). The effect of adenosine analogue (DRB) on a major nucleolar phosphoprotein nucleolin. Biol. Cell *67*, 27–35.

Ochs, R.L., Lischwe, M.A., Spohn, W.H., and Busch, H. (1985). Fibrillarin: a new protein of the nucleolus identified by autoimmune sera. Biol. Cell *54*, 123–134.

Olson, M.O.J. (1990). The role of proteins in nucleolar structure and function. In: The Eukaryotic Nucleus: Molecular Biochemistry and Macromolecular Assemblies 2, ed. P.R. Straus and S.H. Wilson, Caldwell, NJ: Telford Press, 519–559.

Olson, M.O.J., Kirstein, M.N., and Wallace, M.O. (1990). Limited proteolysis as a probe of the conformation and nucleic acid binding regions of nucleolin. Biochemistry *29*, 5682–5686.

Olson, M.O.J., Rivers, Z.M., Thompson, B.A., Kao, W., and Case, S.T. (1983). Interaction of nucleolar phosphoprotein C23 with cloned segments of rat ribosomal deoxyribonucleic acid. Biochemistry *22*, 3345–3351.

Orrick, L.R., Olson, M.O.J., and Busch, H. (1973). Comparison of nucleolar proteins of normal rat liver and Novikoff hepatoma ascites cells by two-dimensional polyacylamide gel electrophoresis. Proc. Natl. Acad. Sci. USA *70*, 1316–1320.

Peculis, B.A., and Gall, J.G. (1992). Localization of the nucleolar protein NO38 in amphibian oocytes. J. Cell Biol. *116*, 1–14.

Pelham, H.R.B., Hardwick, K.G., and Lewis, M.J. (1988). Sorting of soluble ER proteins in yeast. EMBO J. *7*, 1757–1762.

Peter, M., Nakagawa, J., Doree, M., Labbe, J.C., and Nigg, E.A. (1990). Identification of major nucleolar proteins as candidate mitotic substrates of cdc2 kinase. Cell *60*, 791–801.

Query, C.C., Bentley, R.C., and Keene, J.D. (1989). A common RNA motif identified within a defined U1 RNA binding domain of the 70K U1 snRNP protein. Cell *57*, 89–101.

Reimer, G., Pollard, K.M., Penning, C.A., Ochs, R.L., Lischwe, M.A., Busch, H., and Tan, E.M. (1987). Monoclonal autoantibody from a (New Zealand black X New Zealand white)F_1 mouse and some human scleroderma sera target an M_r 34,000 nucleolar protein of the U3 RNP particle. Arthritis Rheum. *30*, 793–800.

Roth, M.B., and Gall, J.G. (1987). Monoclonal antibodies that recognize transcription unit proteins on newt lampbrush chromosomes. J. Cell Biol. *105*, 1047–1054.

Roth, M.B., Zahler, A.M., and Stolk, J.A. (1991). A conserved family of nuclear phosphoproteins localized to sites of polymerase II transcription. J. Cell Biol. *115*, 587–596.

Sapp, M., Richter, A., Weisshart, K., Caizergues-Ferrer, M., Amalric, F., Wallace, M.O., Kirstein, M.N., and Olson, M.O.J. (1989). Characterization of a 48-kDa nucleic-acid-binding fragment of nucleolin. Eur. J. Biochem. *179*, 541–548.

Scheer, U. (1973). Nuclear pore flow rate of ribosomal RNA and chain growth rate of its precursor during oogenesis of *Xenopus laevis*. Dev. Biol. *30*, 13–28.

Siomi, H., Siomi, M., Nussbaum, R.L., and Dreyfuss, G. (1993). The product of the fragile X gene, *FMR1*, has characteristics of an RNA-binding protein. Cell *74*, 291–298.

Sturdier, F.W., Rosenberg, A.H., Dunn, J.J., and Dubendorff, J.W. (1990). Use of T7 RNA polymerase to direct expression of cloned genes. Methods Enzymol. *185*, 60–89.

Swanson, M.S., Nakagawa, T.Y., LeVan, K., and Dreyfuss, G. (1987). Primary structure of human nuclear ribonucleoprotein particle C proteins: conservation of sequence and domain structures in heterogeneous nuclear RNA, mRNA, and pre-rRNA-binding proteins. Mol. Cell. Biol. *7*, 1731–1739.

Wallace, R.A., Jared, D.W., Dumont, J.N., and Sega, M.W. (1973). Protein incorporation by isolated amphibian oocytes: III. Optimum incubation conditions. J. Exp. Zool. *184*, 321–333.